Additive Manufacturing 29 (2019) 100792

Contents lists available at ScienceDirect

Additive Manufacturing

journal homepage: www.elsevier.com/locate/addma

Full Length Article

High-throughput characterization of fluid properties to predict droplet ejection for three-dimensional inkjet printing formulations

Zuoxin Zhou[a], Laura Ruiz Cantu[a], Xuesheng Chen[a], Morgan R. Alexander[b], Clive J. Roberts[b], Richard Hague[a], Christopher Tuck[a], Derek Irvine[a], Ricky Wildman[a,*]

[a] Centre for Additive Manufacturing, Faculty of Engineering, University of Nottingham, Nottingham, United Kingdom
[b] Advanced Materials and Healthcare Technologies, School of Pharmacy, University of Nottingham, Nottingham, NG7 2RD, United Kingdom

ARTICLE INFO

Keywords:
High-throughput screening
Additive manufacturing
3D printing
Inkjet printing
Viscosity
Surface tension
Liquid handler

ABSTRACT

Inkjet printing has been used as an Additive Manufacturing (AM) method to fabricate three-dimensional (3D) structures. However, a lack of materials suitable for inkjet printing poses one of the key challenges that impedes industry from fully adopting this technology. Consequently, many industry sectors are required to spend significant time and resources on formulating new materials for an AM process, instead of focusing on product development. To achieve the spatially controlled deposition of a printed voxel in a predictable and repeatable fashion, a combination of the physical properties of the 'ink' material, print head design, and processing parameters is associated. This study demonstrates the expedited formulation of new inks through the adoption of a high-throughput screening (HTS) approach. Use of a liquid handler containing multi-pipette heads, to rapidly prepare inkjet formulations in a micro-array format, and subsequently measure the viscosity and surface tension for each in a high-throughput manner is reported. This automatic approach is estimated to be 15 times more rapid than conventional methods. The throughput is 96 formulations per 13.1 working hours, including sample preparation and subsequent printability determination. The HTS technique was validated by comparison with conventional viscosity and surface tension measurements, as well as the observation of droplet ejection during inkjet printing processes. Using this approach, a library of 96 acrylate/methacrylate materials was screened to identify the printability of each formulation at different processing temperatures. The methodology and the material database established using this HTS technique will allow academic and industrial users to rapidly select the most ideal formulation to deliver printability and a predicted processing window for a chosen application.

1. Introduction

The use of Additive Manufacturing (AM) to construct three-dimensional (3D) structures layer by layer from pre-designed computer models offers significant advantages over conventional subtractive or formative manufacturing processes. The principal of these is high flexibility in product design and the ability to precisely manufacture complex 3D geometries that have previously been unobtainable [1–4]. There has been interest recently in transforming AM from a prototyping tool towards being used for the direct manufacture of end-use products [5,6]. However, one of the main challenges to achieving this lies in the limited variety of available printable materials when compared to the tens of thousands of polymer materials that have been developed to be processed using conventional polymer processing technologies [4,7,8]. The vast majority of polymer materials incorporated into commercial products are currently processed via conventional methods [9]. To enable a wider range of industry sectors to adopt AM as a main manufacturing route for production, there is an urgent need to identify materials that are fit for purpose. However, despite significant experimental effort there has been limited success, as materials development for AM is often time consuming and extremely multi-disciplinary. This is due to the need for a continuous feedback loop between feedstock preparation, processability of the formulation, curing kinetics, boundary coalescence, dimensional accuracy, surface finish and subsequent evaluation of product performance [10–13].

An important AM processing category is material jetting (or inkjet printing), in which droplets of build materials are selectively deposited [14]. Commercial inkjet 3D printing uses a drop-on-demand process, with either a heater pad or a piezoelectric transducer to trigger ejection of ink droplets from an array of nozzles in the print head. A piezoelectric head is generally more favorable as it allows a wider range of inks to be processed. The movement of the piezoelectric actuator

* Corresponding author.
E-mail address: ricky.wildman@nottingham.ac.uk (R. Wildman).

https://doi.org/10.1016/j.addma.2019.100792
Received 23 January 2019; Received in revised form 4 June 2019; Accepted 8 July 2019
Available online 12 July 2019

produced by an electrical waveform creates a pressure variation in the ink at the nozzle, forcing the ink to form a droplet and subsequently ejecting it from the nozzle [15]. The dominant factors that control the ideal formation and ejection of a droplet of fluid arise from physical properties of the ink and the nozzle geometry. A decrease of nozzle diameter has been found to reduce the number of ink types that are printable, and this observation has been principally related to the influence of the ink viscosity and surface tension.

The printability of an ink is typically assessed using the Fromm's Z parameter (Eq. (1)), which takes into account dynamic viscosity (μ), surface tension (γ), and density (ρ) of the ink, as well as the nozzle diameter (r) [16].

$$Z = \frac{\rho r \gamma}{\mu} \tag{1}$$

Fromm proposed a stable droplet ejection would occur when $Z > 2$ [16]. Reiz and Derby later refined the range to be $1 < Z < 10$ [17] where it was determined that satellite droplets are likely to form if the ink has a Z parameter > 10, and the ink is likely too viscous to be ejected from the nozzle if $Z < 1$. These guidelines can be used to develop new formulations where the inks can be tuned to have a combination of viscosity and surface tension that falls within the 'printable range'. The most commonly used approach to determine viscosity has been oscillatory or capillary rheometers. These measure viscosity via oscillatory movement of a sample liquid between two plates and flow of the liquid through a capillary, respectively. Surface tension is determined by analyzing the droplet shape formed at the terminus of a vertical capillary. However, both methods are time consuming and labor intensive, so neither of these approaches is adequate to rapidly assess a large number of samples.

In order to shorten the development stage of inkjet fluid formulation, this study utilizes HTS to determine the printability of formulations. HTS systems typically involve techniques/apparatus that operate automatically, require very small sample volumes and often allow for simultaneous preparation and testing of multiple samples. In this way, hundreds or thousands of experimental samples can be rapidly screened to identify candidate materials that possess the desired properties. These are often referred to as "hits", from a compound library. HTS has already played an important role in developments within the chemical, pharmaceutical, and biological industries [18–21]. Thus, it was proposed that it may also be a practical and useful approach for the formulation development of AM processes, where the screening of a large number of sample is required.

A recent HTS study used a piezoelectric microarray printer to assess the printability of inkjet formulations based on droplet ejection [22]. However, the microarray printer employed had a different viscosity requirement to many of the commercial inkjet printers, and it did not have the capability to alter the temperature of the cartridge containing the ink. For viscosity measurement, several HTS approaches have been developed, including (1) liquids flowing inside a standard capillary electrophoresis apparatus [23]; (2) falling spheres moving through measuring tubes [24]; (3) the cantilever of atomic force microscope (AFM) in liquids [25]; and (4) aspiration of liquids in pipettes using a liquid handler [26]. In the specific case of the liquid handler, a pressure curve generated during aspiration of the sample into the pipette was used to calculate the dynamic viscosity of the tested liquid [26]. This approach is of interest because (1) it can typically cover the viscosity range required for ejection of an inkjet droplet (normally around 1–30 mPa s); and (2) it does not require a separate cleaning step and (3) only a small volume of samples (< 500 µl) is required [26]. Furthermore, the liquid handler has also been used to automatically determine surface tension of liquids by the integration of a high-precision balance [27], which measures droplet masses generated from a pipette and so correlates that with the surface tension. This HTS approach follows the principle of the stalagmometric method that is one of the most common ways for measuring surface tension [28]. We therefore investigate the suitability of a liquid handler to rapidly determine the printability of a large number of ink formulations that are interesting for 3D inkjet printing.

The first objective of this study was the assessment of accuracy, repeatability and high-throughput capability of the viscosity and surface tension measurement made using a liquid handler. This was followed by the design of a library of 96 ink formulations and the subsequent determination of printability of each formulation at a range of processing temperatures during inkjet printing.

2. Materials and methods

2.1. Materials

Six general-purpose viscosity standards (silicone oils) were used to validate the high-throughput viscosity measurement: S3, S6, N10, S20, N35, and N75 (Paragon Scientific Ltd.). These are Newtonian fluids with viscosities in a range from 3 mPa·s to 125 mPa·s. Surface tension measurement was validated using ethylene glycol (99.8%, 324558, Sigma Aldrich) and isopropanol (≥99.7%, W292907, Sigma Aldrich) aqueous solution. A monomer library of 14 ultraviolet (UV) curable monomers and one polymer were used to form a combinatorial library for a high-throughput printability screening evaluation program. These included 12 functional polymerizable monomer/oligomer used as base materials and another three used as solvent materials. The 12 base materials utilized were bisphenol A ethoxylate diacrylate (BPEODA, 412104, Sigma Aldrich), trimethylolpropane benzoate diacrylate (TMOBDA, 475661, Sigma Aldrich), polycaprolactone dimethacrylate (PCLDMA), 2-hydroxy-3-phenoxypropyl acrylate (HPPA, 407364, Sigma Aldrich), trimethylolpropane ethoxylate triacrylate (TMPETA, 412171, Sigma Aldrich), trimethylolpropane propoxylate triacrylate (TMPOTA, 407577, Sigma Aldrich), bisphenol a glycerolate diacrylate (BAGDA, 411167, Sigma Aldrich), dipentaerythritol penta/heta-acrylate (DPHA), pentaerythritol tetraacrylate (PETTA, 408263, Sigma Aldrich), di(trimethylolpropane) tetraacrylate (DTMPTTA, 408360, Sigma Aldrich), pentaerythritol triacrylate (PETA, 246794, Sigma Aldrich), and tricycle[5.2.1.$0^{2,6}$]decanedimethanol diacrylate (TCDDDA, 496669, Sigma Aldrich). PCLDMA was previously synthesized by attaching photo-reactive groups on PCL-diol following the methods reported in the literature and was determined to have a Mn ~ 1683 g mol^{-1}.[29] Three solvent materials were N-vinylpyrrolidone (NVP, ≥99%, V3409, Sigma Aldrich), 2-hydroxyethyl acrylate (HEA, 292818, Sigma Aldrich), and polyethylene glycol diacrylate (PEGDA, Mn = 250, 475629, Sigma Aldrich).

2.2. Validation of the suitability of using a liquid handler for viscosity measurements

A four-channel liquid handling apparatus (Microlab STARlet, Hamilton Robotics, Inc.) was used to perform high-throughput measurements to determine the printability of ink formulations that were proposed for use in 3D inkjet printing (Fig. 1). The liquid handler utilized air displacement pipetting as the mechanism of operation, which is similar to a handheld electronic pipette system. As the piston moves up within the channel, the air pressure is reduced, and the liquid is aspirated into the tip by the atmosphere pressure at a controlled flow rate. The liquid handler is calibrated by the manufacturer to ensure the flow rate is accurate. Each of the four parallel pipette channels was equipped with a pressure sensor to monitor pressure change during the overall process, i.e. during both aspiration and dispensing of the samples.

To define the suitability of the apparatus for its potential to determine the targeted viscosity measurement, 300 µL of each sample was added into a 96-well polypropylene plate containing 1 mL wells (260252, Thermo Scientific), which was then placed in a heating module at 25 °C. In this initial experiment, eight materials were tested

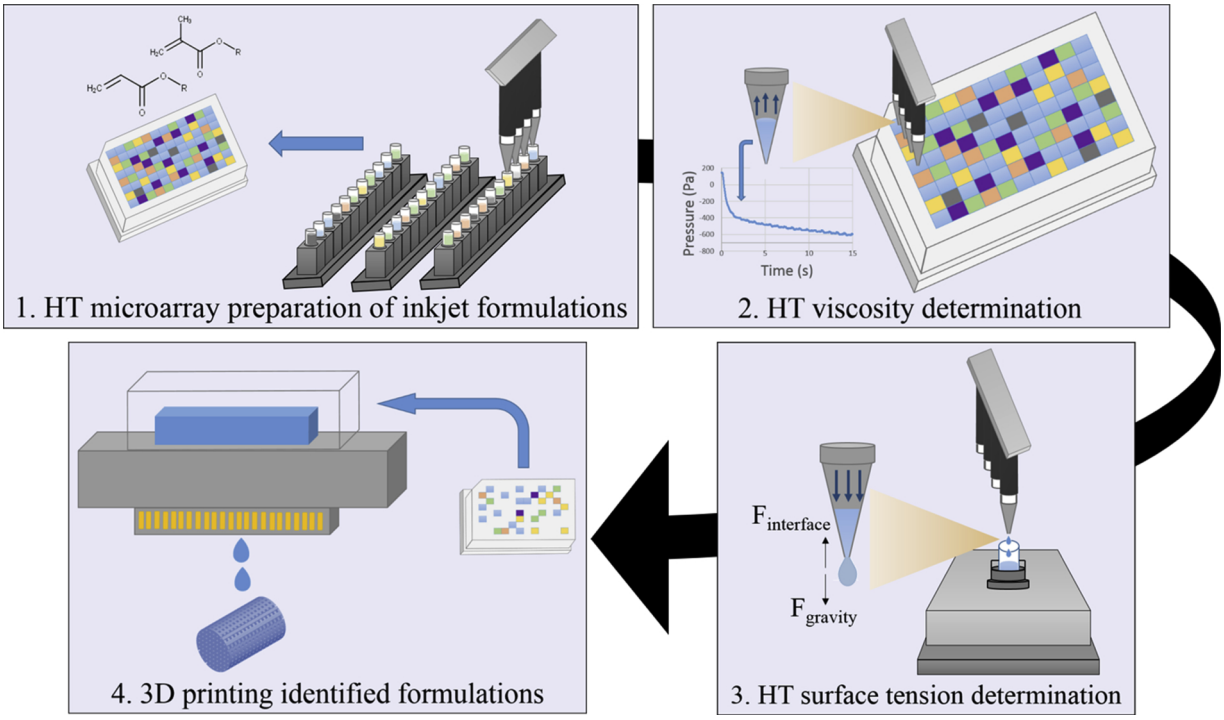

Fig. 1. Schematic illustration of (1) high-throughput microarray preparation of inkjet formulations, high-throughput determination of (2) viscosity and (3) surface tension using the four-channel liquid handling apparatus, and (4) processing the 'hit' formulations with identified printability using an inkjet 3D printing technique.

using a method involving three replicates, where the tested materials included: (1) the six viscosity standards and; (2) PEGDA and TCDDDA. During operation, four samples were simultaneously aspirated into 300 µl pipettes (235902, CO-RE non-filter tips, Hamilton Robotics, Inc.) attached to separate channels on the test head at 10 µl/s for 15 s. The tips followed the reduction in the heights of the samples to ensure that the submerged depth was maintained at 2 mm below the liquid surface. The liquids were then dispensed back into the well plate to minimize material waste during the test. Thereafter, the channels ejected the used pipettes and replaced them with fresh ones, then immediately moved to the next position on the well plate to measure the following four samples. The test was automatically run until completion and where a pressure versus time curve for each aspiration was generated for analysis. The viscosity was then determined from this data using the method detailed in section 2.1.1. and that of the standards (S3, S6, N10, S20, N35, and N75) were compared to the known values at 25 °C. The viscosity determined for the PEGDA and TCDDDA were compared to the values obtained from a conventional oscillatory rheometer (Kinexus Pro, Malvern Instrument). Measurements were performed in an oscillatory shear mode using a cone plate geometer with a 0.2 mm gap. Shear rate sweeps from 10 to 1000 s^{-1} were carried out at 25 °C. At each shear rate, the viscosity was recorded at 5 s intervals within a 180 s testing time. The difference (%) in viscosity was measured using a conventional approach and the high-throughput approach was then obtained.

2.2.1. Calculative procedure to determine viscosity from the aspiration data

The pressure required to maintain a constant aspiration rate depends on the physical properties of the liquid and the geometry of the pipette. In this study, the pipette used was a two-part conical frustum with different angles (**Supplementary Figure 1**). At a given time (t), the radius (R_t) and height (H_t) of the front surface of a liquid aspirated into the bottom part of the pipette were calculated using Eqs. (4) and (5).

$$Qt = \frac{1}{3}\pi H_t (R_t^2 + R_1^2 + R_1 R_t) \tag{2}$$

$$R_1 = 0.2\,mm \tag{3}$$

$$R_t = \left[\frac{\left(\frac{3Qt}{\pi} + 0.1144\right)}{14.2857}\right]^{\frac{1}{3}} \tag{4}$$

$$H_t = \frac{80R_t}{1.4} \tag{5}$$

where Q was the volumetric flow rate. At 10 µl/s, liquid started to flow into the top part of the pipette and the radius (R_t) and height (H_t) were then given by Eqs. (9) and (10).

$$Q(t - 6.12) = \frac{1}{3}\pi (H_t - H_1)(R_t^2 + R_2^2 + R_2 R_t) \tag{6}$$

$$H_1 = 20\,mm \tag{7}$$

$$R_2 = 1.6\,mm \tag{8}$$

$$R_t = \left(\frac{Q(t - 6.12) + \frac{1}{3}\pi \cdot 1.6^2 \cdot 42.62}{\frac{1}{3}\pi \cdot 26.6375}\right)^{1/3} \tag{9}$$

$$H_t = 26.6375 \cdot R_t - 22.62 \tag{10}$$

The pressures of the liquid were subjected to in the tip can be defined using Eq. (11) [26].

$$P_{gas} = P_{flow} - P_{head} - P_{interface} \tag{11}$$

where P_{gas} was gas pressure in the channel, P_{flow} was the pressure drop caused by liquid flowing into the pipette, P_{head} was the difference in the gravitational head pressure between the liquid levels inside and outside the pipette, and $P_{interface}$ was the pressure drop across the interfacial boundary due to the surface tension [26].

The Hagen-Poiseuille equation was used to relate P_{flow} with viscosity of the fluid if each incremented section of the pipette was simplified as a cylindrical pipe. The incremented time was 0.01 s due to the signal frequency of the pressure sensor. A mathematical model was therefore derived to calculate P_{gas} (Eq. (15)).

Control		10 v/v % solvent			20 v/v % solvent			30 v/v % solvent			40 v/v % solvent		
		NVP	HEA	PEGDA	NVP	HEA	PEGDA	NVP	HEA	PEGDA	NVP	HEA	PEGDA
BPEODA	A1	B1	C1	D1	E1	F1	G1						
TMOBDA	H1	A2	B2	C2	D2	E2	F2						
PCLDMA	G2	H2	A3	B3	C3	D3	E3						
HPPA	F3	G3	H3	A4	B4	C4	D4						
TMPETA	E4	F4	G4	H4	A5	B5	C5						
TMPOTA	D5	E5	F5	G5	H5	A6	B6						
PETTA	C6	D6	E6	F6	G6	H6	A7						
DTMPTTA	B7	C7	D7	E7	F7	G7	H7						
PETA	A8	B8	C8	D8	E8	F8	G8						
TCDDDA	H8	A9	B9	C9	D9	E9	F9						
BAGDA	G9	H9	A10	B10	C10	D10	E10	F10	G10	H10	A11	B11	C11
DPHA	D11	E11	F11	G11	H11	A12	B12	C12	D12	E12	F12	G12	H12

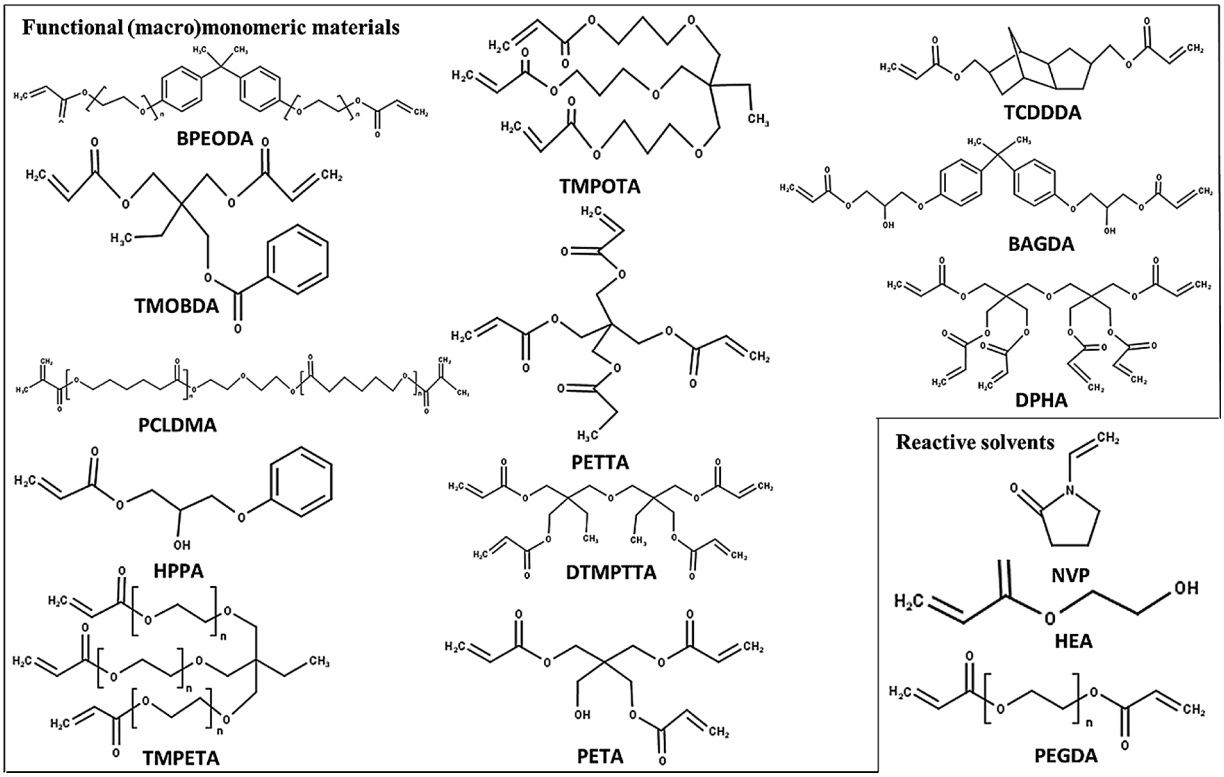

Fig. 2. Arrangement of the library of inkjet formulations in a 96-well plate and the chemical structures of the functional (macro)monomeric materials and reactive solvents.

$$P_{flow} = \int_0^H \frac{8\mu Q}{\pi\left(\frac{R_t + R_{(t-0.01)}}{2}\right)^4} dH \tag{12}$$

$$P_{head} = \rho g(0.02 - H_t) \tag{13}$$

$$P_{interface} = \frac{2\gamma\cos\theta}{R_t} \tag{14}$$

$$P_{gas} = \int_0^H \frac{8\mu Q}{\pi\left(\frac{R_t + R_{(t-0.01)}}{2}\right)^4} dH - \rho g(0.02 - H_t) - \frac{2\gamma\cos\theta}{R_t} \tag{15}$$

where μ was dynamic viscosity, ρ was density, g was gravity of earth, γ was surface tension, and θ was contact angle of the liquid with the pipette surface.

A mathematical model was generated using MATLAB 2016a (MathWorks, Inc.) to fit the experimental pressure (P_{gas}) vs. time data. The sum of the square of the residual between experiment and analytical expression was taken as a minimization objective; experimental parameters, such as pressures and time, were taken as variables. MATLAB was used to apply a least-square method was applied to minimise the objective. The computation was performed with MATLAB 2016a on a personal computer. Curve fitting was performed between 10 and 15 s as a consequence of the actual volumetric flow rate not being sufficiently accurate during the transient stage when the liquid starts to aspirate into the pipette. The influence of $P_{interface}$ is small in comparison to the other contributions beyond the transients prior to 10 s and as a consequence the terms incorporating the surface tension and contact angle were neglected during the curve fitting procedure. With a known density, the viscosity was determined using the curve fitting to best fit to the experimental data.

2.3. Procedure for the validation of the suitability of using a liquid handler for surface tension measurements in the desired range

A high-precision balance (WXS205SDUV/15, Mettler Toledo) which was integrated into the STARlet liquid handler and was used to facilitate surface tension measurement. 110 µl of a sample liquid was aspirated to a 300 µl pipette, which was then moved to the position above the balance. Once in position, it started to dispense the sample at 5 µl/s for 20 s. Readings of the balance were recorded by the proprietary LVK software (Hamilton Robotics, Inc.) at 20 Hz. Once data collection was complete, the channel on the test head ejected a used pipette which was then replaced ready for measurement of the next sample. This test was automatically repeated until all the samples were measured.

2.3.1. Calculative procedure to determine surface tension

Determination of the surface tension was based on the evaluation the equilibrium of the weight force F_w and the adhesive force F_A when the drop detaches from the tip via the relationship defined in Eq. (16) [27]. Using water as a reference sample with a known surface tension, the surface tension of a sample is calculated (Eq. (17)).

$$F_w = F_A = 2\pi r\gamma f_{inst} \tag{16}$$

$$\gamma_{sample} = m_{sample}\frac{\gamma_{water}}{m_{water}} \tag{17}$$

where: r is the interfacial radius, f_{inst} is the correction factor, γ is the surface tension, and m is the droplet mass.

Nine samples were tested using both a high-throughput approach and a conventional drop shape analysis approach, these test materials were: (1) ethylene glycol aqueous solution at 100, 75, 50 and 25 wt.%; (2) isopropanol aqueous solution at 100, 75, 50, and 25 wt.%; and (3) purified water. A drop shape analyzer (DSSA100S, KRÜSS GmbH Germany) was used to measure the dimensions of each sample using a pendant drop method. Surface tension was determined using the software of the equipment based from the Young-Laplace fit to the contour of a pendant droplet hanging on the tip of a pipette. A comparison of the difference (%) in value of the surface tension measured using both conventional and high-throughput approaches for each sample was then obtained.

2.4. General procedure for the preparation and screening of a library of inkjet formulations for potential printability

The HTS method was used to rapidly determine the potential for inkjet printability of a number of target polymeric ink formulations at different temperatures, with up to 96 materials being assessed in a single microarray. A library was designed by mixing one of 12 (macro) monomeric materials as the "functional" base component of the ink with each of the other 3 reactive solvent materials (Fig. 2). These reactive solvents all contain photo-reactive groups, able to be polymerized quickly upon deposition from the inkjet print head when a photoinitiator is included in the ink formulation. Each base material was mixed with a solvent at 80, 90 and 100 v/v %. In the specific cases of BAGDA and DPHA, 60 and 70 v/v % were also prepared due to their high viscosities. Overall, a library of 96 inkjet formulations was designed to undergo HTS evaluation of printability.

The selected inks therefore contained acrylate/methacrylate (macro)monomers which produce polymers which have desirable materials properties. The specific polymers were chosen as they demonstrate promising material functionalities, including: (1) bacterial attachment; [20] (2) bioresorption [29]; (3) interfacial compatibility with electrodes [30]; (4) chemical stability [31]; (5) tribological properties [32]; and (3) controlled drug delivery [33,34]. All the monomeric components that may result in functional polymers were shown not to be inkjet printable at 30 °C due to their viscosities being outside the jettable range. Thus, the reactive solvents, i.e. NVP, HEA, and PEGDA, were added to reduce the viscosity and act as a photo-polymerize/crosslink agents under UV radiation. The polymerized compounds of NVP, HEA and PEGDA are biocompatible. Additionally, poly(vinyl pyrrolidone) (PVP), poly (2-hydroxyethyl acrylate) (PHEA) and PEGDA are capable of increasing the hydrophilicity of acrylate/methacrylate polymers that are often hydrophobic.

Each reagent was transferred to a 1.5 ml polypropylene flip tube (235692, Hamilton Robotics, Inc.), and loaded into a FlipTube Sample carrier (809030, Hamilton Robotics, Inc.) in the deck of the liquid handler. Materials were then automatically transferred to the 96-well plate containing wells of 1 ml volume using the liquid handler. The combination of reagents that constituted each sample mixture were added so that there was at 500 µl in each well to ensure sufficient volume for testing. A mixing cycle was added to the last step of each sample preparation. The pipette was used to aspirate and dispense back 250 µl from the mixture for 10 times to promote mixing. The viscosity measurements were then made using the experimental method described in Section 2.2. The viscosity measurements were performed at 30, 40, 50, 60 and 70 °C to cover the range of processing temperatures for an inkjet printhead. This was achieved by heating the well-plate to each testing temperature using the integrated heating module. The temperature was checked using a thermometer before measurement.

Surface tension was only measured at 30 °C because it was observed in the viability screening (Section 2.3.1) that there was no significant change exhibited over the temperature range of interest. However, some of the test samples that demonstrated highly viscous properties were tested at higher temperatures to ensure that the pressure required to dispense the sample was below the operable limit of the apparatus.

The Z parameter was subsequently calculated using the experimental data to predict the printability of each formulation in the library (Eq. (1)).

2.5. General procedure for the jetting of droplets using a 3D inkjet printer

The formulations containing each functional base material at 80 v/v % with PEGDA as the solvent were used to demonstrate printability in a Dimatix DMP-2830 inkjet printer (Fujifilm). 3 ml of the ink was filtered and ejected into a 10 pl drop volume Dimatix cartridge (Fujifilm). The cartridge was covered with foil tape to avoid ambient UV effects. The cartridge was then heated to different temperatures and subsequently ejected droplets using a standard waveform programme. Droplet ejection was recorded using the internal camera. The droplet ejection was then compared with the HTS results to demonstrate the reliability of this approach.

3. Results and discussion

3.1. Validation of the HTS

The pressure vs. time curve generated from the predictive analytical model (Fig. 3) was compared with and shown to fit well with the experimentally generated curve. The R^2 values for both sets of data were > 0.99 in the region used for curve fitting (10 s < t < 15 s). Furthermore, the viscosity measurement using the HTS method were found to be highly comparable with those measured using the conventional oscillatory rheometer. All data were demonstrated to be close to the reference line with a slope of 1 and an offset of 0, indicating how comparable results were from these two approaches. With one exception, all of the data were found to agree within +/-10% between the two approaches, the exception being S3 recorded a 14.62%, S3 had the lowest viscosity of all samples being tested. For fluids with lower viscosities, P_{head} is a more dominant factor in the analytical model compared to P_{flow} (Eq. (11)), and vice versa for high viscosities. The presented HTS approach demonstrated a sufficient level of accuracy to be regarded as capable of determining the viscosity of Newtonian fluids in this set viscosity range, because the viscosities of Newtonian fluids

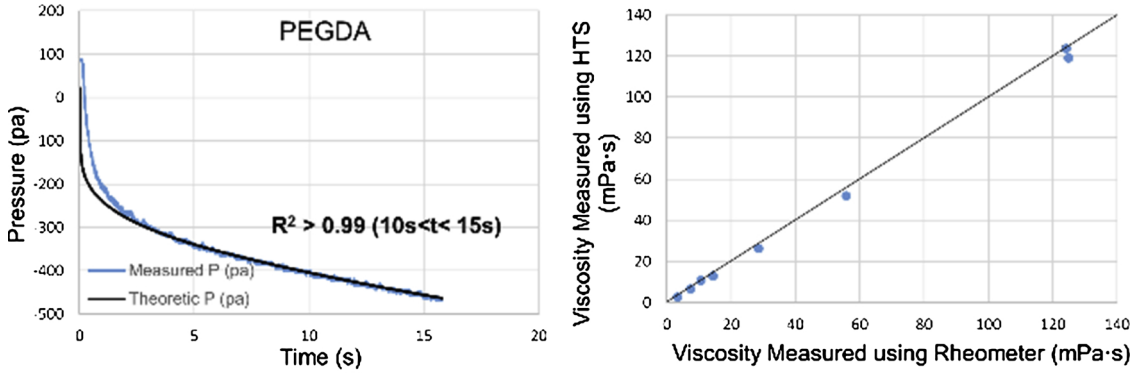

	Viscosity (mPa·s) @ 25°C		
	Measured using Rheometer	Measured using HTS	Difference
PEGDA250	10.52	10.94±0.10	3.99%
TCDDDA	124.08	123.70±1.13	0.30%
S3	3.26	2.78±0.08	14.62%
S6	7.37	6.73±0.16	8.68%
N10	14.26	13.07±0.15	8.37%
S20	28.39	26.37±0.19	7.12%
N35	55.70	52.07±0.13	6.52%
N75	124.80	119.06±0.21	4.60%

Fig. 3. Comparison of the viscosities measured using oscillatory rheometer and HTS at 25 °C. An example (top left) was given to demonstrate the accuracy of the analytical model to the experimental data.

are not affected by shear rate. This is important because, at a fixed volumetric flow rate, a fluid was subjected to different shear rates during the aspiration process and therefore this factor could be neglected for Newtonian fluids. The rheometer data of the (macro) monomer mixtures tested in this study confirmed that they all exhibited Newtonian behavior. Additionally, the viscosity standards were specifically chosen as they were known to be Newtonian fluids and thus their viscosities could be directly compared with those obtained from the HTS tests. Monomers and very low molecular weight polymers are typically used in the preparation of inkjet formulations and sine these are small isotropic molecules they are not easily oriented by flow. These low molecular weight polymers are often referred to as oligomers or as in this case when they have a polymerizable groups in their structure they are referred to as macromonomers. Screening non-Newtonian fluids is possible by either adopting a priori non-Newtonian descriptors and relations or by combining the approach with computational fluid dynamics methods [26]. Due to the high sensitivity of the pressure transducer equipped within each channel of the liquid handler, the viscosity can be determined directly after the point at which the flow rate reaches equilibrium. The maximum pressure attainable with the liquid handler used in this study was approximately 4500 Pa, which was associated with a viscosity of ˜ 270 mPa·s. This is sufficient for the work intended for this study because the upper limit of viscosity for inkjet printing is in a range of 20–40 mPa s, depending on the surface tension and density of the ink. Thus, any test liquid demonstrating a viscosity beyond the measurement of HTS approach was classified as 'not printable'. Under the current setup, only 200 µl of liquid was required for the viscosity measurement and it can be recycled after the test, which was an advantage over approaches such as the use of cone and plate rheometry. The 96 multi-well array format was shown to have the dual benefits of enabling miniaturization and avoiding cross contamination.

Surface tension measurements using HTS matched well with those of the comparable conventional approach (Fig. 4). Tested samples demonstrated surface tension across a wide range, i.e. from 20 mN/m to 70 mN/m. The differences between the two approaches were all observed to be within 6%, with half of the tested samples being within 3%. Again, all data was observed to sit close to the reference line with a slope of 1 and an offset of 0, indicating the accuracy of surface tension measurements using HTS. For each measurement lasting 20 s, a minimum 5 droplets were generated giving sufficient replicates. Deviation was within ± 0.3% of the average value based on the replicates of the same sample, which demonstrated excellent testing repeatability. The measurement of surface tension is fully automatic for pipetting liquids in a sequence into the vial that is sitting on the balance. The minimum amount of liquid required for surface tension measurement is a droplet-size.

3.2. Determination of inkjet printability for a library of formulations

After the validation of the HTS methods for viscosity and surface tension measurements, a high-throughput determination of the inkjet printability of a microarray of acrylate/methacrylate formulations was conducted. Overall, the program included 480 measurements of viscosity (96 samples times 5 temperatures) (Fig. 5) and 96 measurements of surface tension (Fig. 6). The viscosities of all 12 functional (macro) monomeric materials reduced after adding each of the three reactive solvents, indicating an increase in the likelihood of achieving printability. A variety of properties can be influenced by the selection of different reactive solvents. PHEA is one of the most hydrophilic materials amongst the group of acrylate/methacrylate polymers and therefore can be used to form a hydrogel network. However, since it only contains one polymerizable vinyl group will not lead to a crosslinking but rather will result in a thermoplastic. PEGDA is hydrophilic and has good molecular flexibility in rotational movement of the chain segments resulting in mechanically toughening other materials [35,36]. However, PEGDA has two vinyl groups so is likely to produce a thermoset. PVP is again a thermoplastic (i.e. the monomer contains only one vinyl group) which is soluble in a broad range of organic solvents and used in a wide range of medical, pharmaceutical, and cosmetic applications [37]. The surface tension of all the (macro)monomers remained in a range of 30–40 mN/m after solvent addition, which is ideal for inkjet printing. Thus, the Z-parameter was then determined across a temperature of 30–70 °C which is the typical range for most commercial

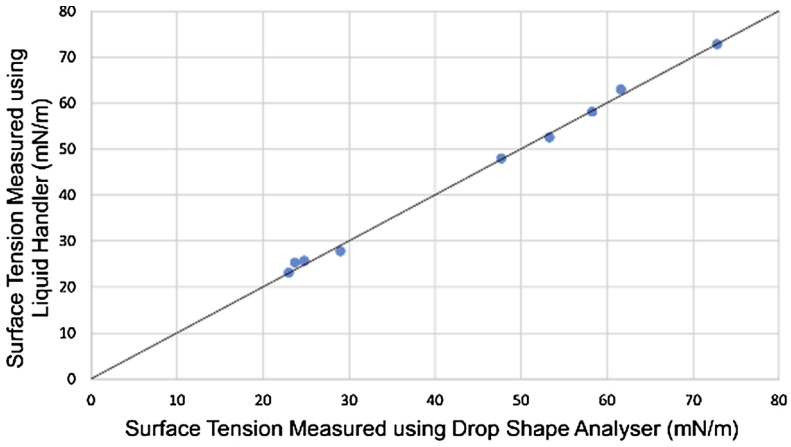

		Surface Tension (mN/m)		
		HTS	Pendant Drop	Difference
Water		Used as a reference		
Ethylene glycol aqueous solution	100wt.%	47.43±0.10	47.70	0.57%
	75wt.%	52.00±0.08	53.30	2.43%
	50wt.%	57.45±0.16	58.26	1.39%
	25wt.%	62.30±0.21	61.63	1.09%
Isopropanol aqueous solution	100wt.%	22.94±0.20	23.00	0.27%
	75wt.%	25.03±0.16	23.74	5.44%
	50wt.%	25.49±0.17	24.79	2.81%
	25wt.%	27.79±0.10	29.00	4.35%

Fig. 4. Comparison of the surface tensions measured using drop shape analyzer and HTS.

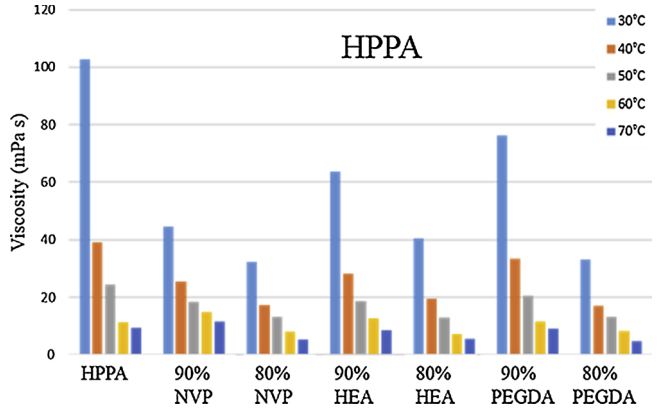

Fig. 5. Viscosities measured using HTS for the library of inkjet formulations at 30–70 °C. HPPA-based formulations are presented as examples. The complete viscosity results of the library are included in Supplementary Figure 2 and Supplementary Figure 3.

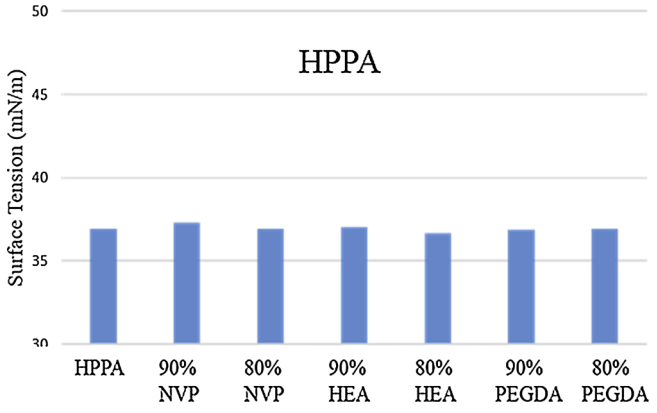

Fig. 6. Surface tensions measured using HTS for the library of inkjet formulations. HPPA-based formulations are presented as examples. The complete surface tension results of the library are included in Supplementary Figure 4 and Supplementary Figure 5.

printer cartridges (Fig. 7). At 30 °C, only one formulation (80% TCDDDA in NVP) was identified as 'printable', as all the other 95 formulations had a Z-parameter lower than 1 which suggests they were too viscous to form droplets that can be ejected from a piezoelectric head with 20 μm nozzle diameter. Viscosities decreased with an increase in the well temperature, resulting in more formulations exhibiting solutions that would be printable. However, half of the functional (macro) monomeric materials were still outside the printable range at 70 °C, indicating the necessity of adding an additional solvent (either reactive or organic) to further reduce their viscosities.

None of the tested formulations had Z-parameter above 10, and therefore it was predicted that satellite droplets would not be formed.

3.3. Assessment of formulations in processing

The experimental printability of specific ink formulation successfully identified as exhibiting the correct characteristics by the HTS routes was then validated using a Dimatix inkjet printer to process these formulations at different temperatures (Fig. 8). Ideal droplet formation was observed for HPPA, PETTA, and DTMPTTA (80% in PEGDA) at

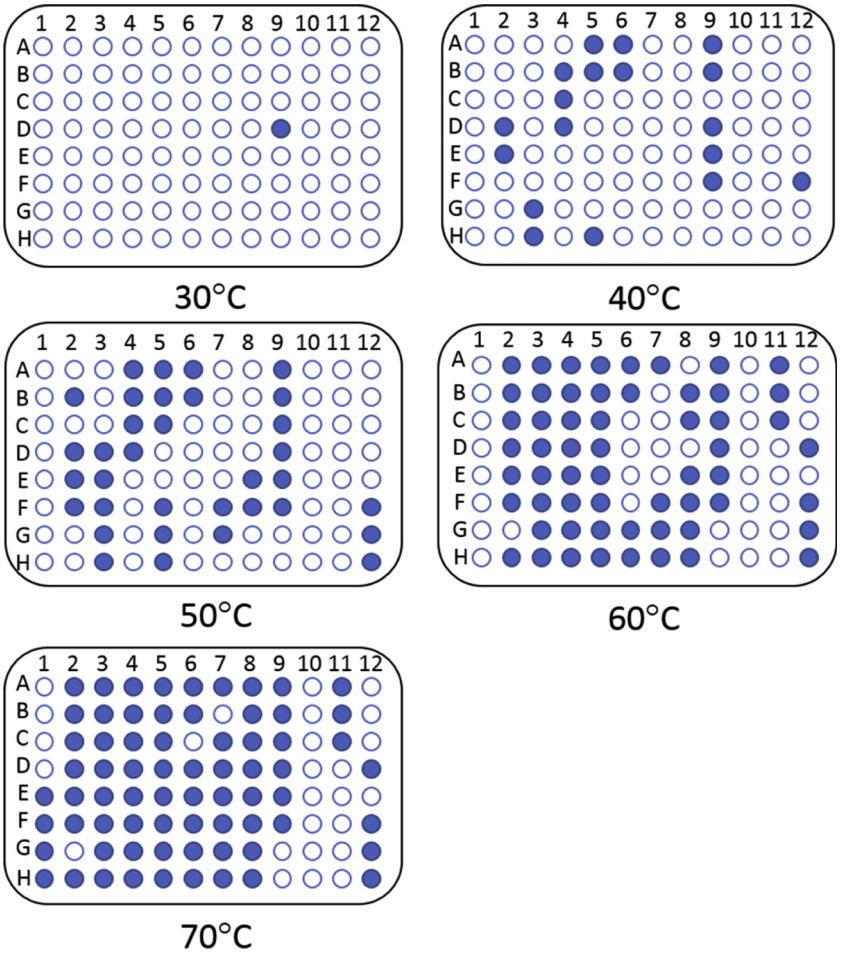

Fig. 7. Determination of inkjet printability for the library of inkjet formulations at 30–70 °C. Candidates with identified printability ($1 < Z < 10$) were shown as solid blue (For interpretation of the references to colour in this figure legend, the reader is referred to the web version of this article.).

40 °C, 60 °C, and 60 °C, respectively, which was identified in the HTS as the minimum processing temperature for each of these formulations. The head of the droplet left the nozzle within 200 ms after it appeared. As expected, because the Z parameter was determined in an ideal range, the droplets were observed to drag a long tail but this did not breakup into satellite droplets. Droplet ejection did not occur for the same formulations if they were processed at 10 °C lower, due to the viscous dissipation and energy associated with surface formation being too great for the pressure pulses generated from the superposition of acoustic waves. This observation suggests the key result that the printability determined using HTS translates well to the actual printing performance of formulations. The overall steps for a complete inkjet formulation development include (1) design of a library, (2) preparation of candidate samples, (3) characterization of ink properties to predict droplet ejection, (4) optimization of processing parameter to achieve good droplet coalesce, and (5) polymerization to form solid 3D structures. This study has specifically targeted step 2 and 3, which are the vital steps to determine if a droplet can be ejected or not. It is also the most time-consuming step in the overall formulation development for inkjet processing. Using the HTS method developed in this study candidate samples that exhibit reliable droplet ejection can be rapidly screened and identified. This then can provide a platform for investigate processing parameters and polymerization for the identified candidate samples. Ink stability may also affect printability, such as when an ink formulation contains volatile solvents or solids. However, no HTS technique or method has been yet developed to increase throughput and efficiency of these tests. Therefore, it is suggested to use conventional ways of testing to perform further investigation, which is beyond the scope of this study.

3.4. Quantification of time saving from the high-throughput system

A comparison of the overall time required to complete such a testing program were estimated between HTS and conventional approaches (Table 1) was then conducted by recording the processing time at each step during practical work. The estimated time required for HTS includes pipette pick-up and removal, as well as channel travelling between different hardware testing stations within the liquid handler. From this assessment the HTS is estimated to be 15 times more rapid than the conventional approaches, with an additional advantage of being fully automated. With the current setup, the throughput of this approach is 96 formulations per 13.1 working hours. The throughput could be further increased if a liquid handler with more channels was used. The HTS proposed in this study provided a predictive power that can be adopted by both academic and industry. The implementation of this approach can potentially revolutionize the current situation in the development of 3D printing formulations.

4. Conclusions

A high-throughput approach for the identification of printable ink formulations to be used for inkjet 3D printing has been developed using a one-stop liquid handling station. The method involved a series of integrated, fully automated steps, including a) automatic preparation of micro-arrays, b) viscosity measurement at different processing temperatures, and c) surface tension measurement. Method testing with

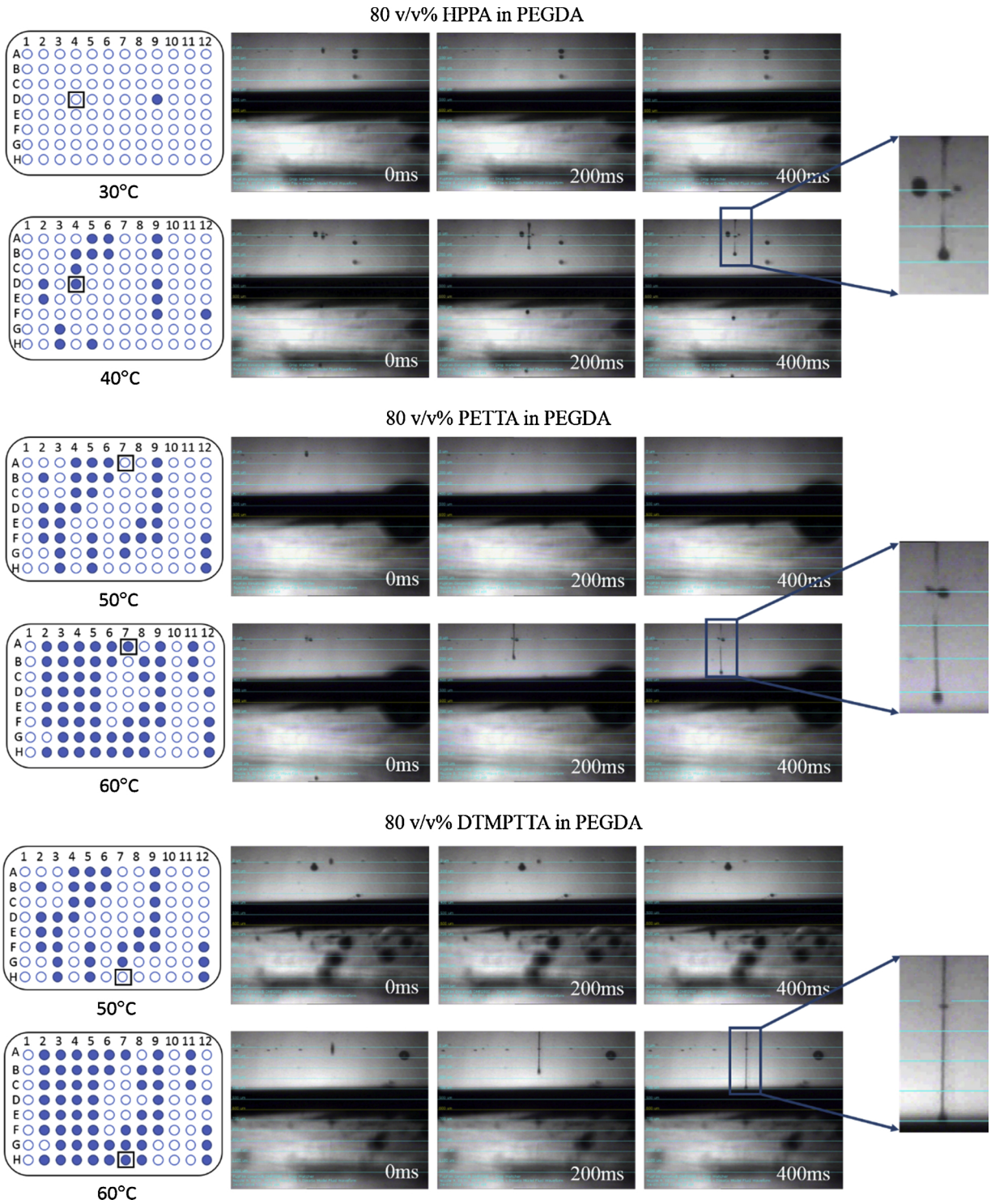

Fig. 8. Droplet ejection captured using an internal camera within a Dimatix inkjet printer, at an interval of 0, 200, and 400 ms. Candidate samples were printed at two temperatures that were identified as 'printable' and 'not printable' from the HTS results. Positions in the array are highlighted in black squares.

Table 1
The estimated time breakdown that is needed to determine inkjet printability for 96 samples, using conventional approaches and HTS.

	96 Sample Preparation			Viscosity Measurement		Surface Tension Measurement	Overall Time
	Sample Loading	Microarray Preparation	Agitation	Temperature Settling	Testing	Testing	
Conventional Approaches	2 min × 96		15 min × 96	5 min × 96 × 5	15 min × 96 × 5	5 min × 96	195.2 h
HTS	2 min × 96	20 min	60 min	30 min × 5	1.75 min × 24 × 5	1 min × 96	13.1 h

idealized materials demonstrated that the HTS results were closely matched to those using conventional testing approaches. A rapid screening program was performed on a library of 96 inkjet formulations which were mixtures of highly viscous functional (macro)monomer materials with reactive solvents. The method was then used to successfully assess the potential printability of the 96 formulations and also defined the ideal processing temperature window for each of ink. The printability of formulations were subsequently assessed in inkjet processes, which confirmed the reliability of the HTS prediction of printability.

An assessment of the time saving that the HTS method bestows was then made and estimated to be 15 times more rapid than the conventional approaches, with an additional advantage of being fully automated. This advantage could be further increased if a liquid handler with more channels was used. Thus, the HTS method and apparatus proposed in this study clearly provided a predictive capability that can be adopted by both academia and industry to greatly increase the success rate in identifying usable inkjet printing inks. The rapid identification of inks can apply to screen molecular descriptor and study chemical-activity in modern drug and biomaterial discovery.

Associated content

Cross-sectional structure of the pipette; full viscosity measurement; full surface tension measurement.

This material is available free of charge via the Internet at http://pubs.acs.org."

Author contributions

The manuscript was written through the contribution of all the authors. Z.Z. carried out the bulk of the experimental work, data analysis, and manuscript preparation. The library of inkjet formulations was designed by Z.Z. and L.R.-C. The Matlab script was coded by X.C. The work was conceived, organised, and made possible with funding gained by M.R.A., C.J.R., R.H., C.T., D.J.I., and R.W.

Notes

The Authors declare no competing financial interest.

Acknowledgments

The authors acknowledge funding from the EPSRC (Engineering and Physical Sciences Research Council) via research grant EP/N024818/1 titled 'Formulation for 3D Printing: Creating a Plug and Play Platform for a Disruptive UK Industry'.

References

[1] M.S. Saleh, J. Li, J. Park, R. Panat, 3D printed hierarchically-porous microlattice electrode materials for exceptionally high specific capacity and areal capacity lithium ion batteries, Addit. Manuf. 23 (2018) 70–78.
[2] A. Bandyopadhyay, K.D. Traxel, Invited review article: metal-additive manufacturing—modeling strategies for application-optimized designs, Addit. Manuf. 22 (2018) 758–774.
[3] T. Primo, M. Calabrese, A. Del Prete, A. Anglani, Additive manufacturing integration with topology optimization methodology for innovative product design, Int. J. Adv. Manuf. Technol. 93 (2017) 467–479.
[4] F.P.W. Melchels, et al., Additive manufacturing of tissues and organs, Prog. Polym. Sci. 37 (2012) 1079–1104.
[5] S.A.M. Tofail, et al., Additive manufacturing: scientific and technological challenges, market uptake and opportunities, Mater. Today 21 (2018) 22–37.
[6] D.R. Eyers, A.T. Potter, Industrial additive manufacturing: a manufacturing systems perspective, Comput. Ind. 92–93 (2017) 208–218.
[7] K.V. Wong, A. Hernandez, A review of additive manufacturing, ISRN Mech. Eng. 2012 (2012) 1–10.
[8] Z. Zhou, et al., Effects of poly (ε-caprolactone) coating on the properties of three-dimensional printed porous structures, J. Mech. Behav. Biomed. Mater. 70 (2017) 68–83.
[9] R.D. Goodridge, C.J. Tuck, R.J.M. Hague, Laser sintering of polyamides and other polymers, Prog. Mater. Sci. 57 (2012) 229–267.
[10] A. Butscher, et al., Printability of calcium phosphate powders for three-dimensional printing of tissue engineering scaffolds, Acta Biomater. 8 (2012) 373–385.
[11] Z. Zhou, F. Buchanan, C. Mitchell, N. Dunne, Printability of calcium phosphate: calcium sulfate powders for the application of tissue engineered bone scaffolds using the 3D printing technique, Mater. Sci. Eng. C 38 (2014) 1–10.
[12] C. Sturgess, C.J. Tuck, I.A. Ashcroft, R.D. Wildman, 3D reactive inkjet printing of polydimethylsiloxane, J. Mater. Chem. C 5 (2017) 9733–9745.
[13] Z. Zhou, et al., Development of three-dimensional printing polymer-ceramic scaffolds with enhanced compressive properties and tuneable resorption, Mater. Sci. Eng. C 93 (2018) 975–986, https://doi.org/10.1016/j.msec.2018.08.048.
[14] ASTM International, F2792-12a - Standard Terminology for Additive Manufacturing Technologies, Rapid Manuf. Assoc., 2013, pp. 10–12, https://doi.org/10.1520/F2792-12A.2.
[15] H.P. Le, Progress and trends in ink-jet printing technology, J. Imaging Sci. Technol. (1998) doi:citeulike-article-id:3979011.
[16] J.E. Fromm, Numerical calculation of the fluid dynamics of drop-on-demand jets, IBM J. Res. Dev. 28 (1984) 322–333.
[17] N. Reis, B. Derby, Ink jet deposition of ceramic suspensions: modeling and experiments of droplet formation, MRS Proc. 625 (2000) 117.
[18] T.S. Klann, et al., CRISPR-Cas9 epigenome editing enables high-throughput screening for functional regulatory elements in the human genome, Nat. Biotechnol. 35 (2017) 561–568.
[19] R. Macarron, et al., Impact of high-throughput screening, Nature 10 (2011) 188–195.
[20] A.L. Hook, et al., Combinatorial discovery of polymers resistant to bacterial attachment, Nat. Biotechnol. 30 (2012) 868–875.
[21] R. Patwardhan, High-resolution analysis of DNA regulatory elements by synthetic saturation mutagenesis, Dana 27 (2010) 1173–1175.
[22] I. Louzao, et al., Identification of novel 'inks' for 3D printing using high-throughput screening: bioresorbable photocurable polymers for controlled drug delivery, ACS Appl. Mater. Interfaces 10 (2018) 6841–6848.
[23] A. Allmendinger, et al., High-throughput viscosity measurement using capillary electrophoresis instrumentation and its application to protein formulation, J. Pharm. Biomed. Anal. 99 (2014) 51–58.
[24] J. Ma, J.M. Lopez-Pedrosa, M. Bradley, High-throughput viscosity determinations, Rev. Sci. Instrum. 79 (2008).
[25] N. Ahmed, D.F. Nino, V.T. Moy, Measurement of solution viscosity by atomic force microscopy, Rev. Sci. Instrum. 72 (2001) 2731–2734.
[26] S. Deshmukh, et al., A novel high-throughput viscometer, ACS Comb. Sci. 18 (2016) 405–414.
[27] S. Amrhein, S. Suhm, J. Hubbuch, Surface tension determination by means of liquid handling stations, Eng. Life Sci. 16 (2018) 532–537.
[28] T. Tate, On the magnitude of a drop of liquid formed under different circumstances, London, Edinburgh, Dublin Philos. Mag. J. Sci. (1864), https://doi.org/10.1080/14786446408643645.
[29] Y. He, et al., A new photocrosslinkable polycaprolactone-based ink for three-dimensional inkjet printing, J. Biomed. Mater. Res. - Part B Appl. Biomater. 105 (2017) 1645–1657.
[30] K. Liu, et al., A cross-linking succinonitrile-based composite polymer electrolyte with uniformly dispersed vinyl-functionalized SiO2Particles for Li-Ion batteries, ACS Appl. Mater. Interfaces 8 (2016) 23668–23675.
[31] J. Ma, et al., Dipentaerythritol penta-/hexa-acrylate based-highly cross-linked hybrid monolithic column: preparation and its applications for ultrahigh efficiency separation of proteins, Anal. Chim. Acta 963 (2017) 143–152.
[32] Y.K. Cho, S.H. Hwang, Diisocyanate type effects on flexibility and coating performance of UV-curable hard coatings based on tetrafunctional urethane acrylates, Polym. Bull. (2018) 1–13, https://doi.org/10.1007/s00289-018-2363-5.
[33] W. Yan, et al., Towards nanoporous polymer thin film-based drug delivery systems, Thin Solid Films 517 (2009) 1794–1798.
[34] X. Zhan, G. Tang, S. Chen, Z. Mao, A new copolymer membrane controlling clonidine linear release in a transdermal drug delivery system, Int. J. Pharm. 322 (2006) 1–5.
[35] D. Yao, T. Kuila, K.B. Sun, N.H. Kim, J.H. Lee, Effect of reactive poly(ethylene glycol) flexible chains on curing kinetics and impact properties of bisphenol-a glycidyl ether epoxy, J. Appl. Polym. Sci. (2012), https://doi.org/10.1002/app.35275.
[36] A. Vonarbourg, C. Passirani, P. Saulnier, J.P. Benoit, Parameters influencing the stealthiness of colloidal drug delivery systems, Biomaterials (2006), https://doi.org/10.1016/j.biomaterials.2006.03.039.
[37] M. Teodorescu, M. Bercea, Poly(vinylpyrrolidone) – a versatile polymer for biomedical and beyond medical applications, Polym. - Plast. Technol. Eng. (2015), https://doi.org/10.1080/03602559.2014.979506.